The Journal of Experimental Biology 206, 1397-1408

doi:10.1242/jeb.00264

Comparative equilibrium mechanical properties of bovine and lamprey cartilaginous tissues

Hayden-William Courtland[1], Glenda M. Wright[1], Robert G. Root[2] and M. Edwin DeMont[3,*]

[1]*Department of Biomedical Sciences, UPEI Atlantic Veterinary College, Charlottetown, Prince Edward Island, C1A 4P3, Canada,* [2]*Department of Mathematics, Lafayette College, Easton, PA 18042, USA* and [3]*Department of Biology, St Francis Xavier University, Antigonish, Nova Scotia, B2G 2W5, Canada*

*Author for correspondence (e-mail: edemont@stfx.ca)

Accepted 27 January 2003

Summary

In contrast to all other vertebrate cartilages, the major extracellular matrix protein of lamprey cartilages is not collagen. Instead, there exists a unique family of noncollagenous structural proteins, the significance of which is not completely understood. A custom-built uniaxial testing apparatus was used to quantify and compare equilibrium stress-relaxation behavior (equilibrium moduli, stress decay behavior, recovery times and relaxation times) of (1) lamprey pericardial cartilages with perichondria tested in tension (young adult and aged), (2) annular cartilages without perichondria tested in compression (young adult and aged) and (3) bovine auricular cartilage samples without perichondria tested in both tension and compression. Results of this study demonstrated that all cartilages were highly viscoelastic but with varying relaxation times; approximately 120 min for annular and pericardial cartilages and 30 min for bovine auricular cartilages. For mean equilibrium moduli, young adult lamprey annular cartilages (0.71 MPa) and pericardial cartilages (2.87 MPa) were found to be statistically different. The mean moduli of all bovine auricular cartilages were statistically identical to lamprey cartilages except in the case of aged adult pericardial cartilages, which were statistically larger than all other cartilages at 4.85 MPa. Taken together, the results of this study suggest that lamprey cartilages are able to exhibit mechanical properties largely similar to those of mammalian cartilages despite unique structural proteins and differences in extracellular matrix organization.

Key words: cartilage, collagen, tension, compression, lamprey, *Petromyzon marinus*, stiffness, viscoelastic properties.

Introduction

Characterized by the absence of jaws, scales and paired fins, the parasitic sea lamprey are markedly different from the other major division of vertebrates, Gnathostomata (Hubbs and Potter, 1971). In addition, bone is completely absent from lamprey; instead cartilage forms the major supporting structure. The annular cartilage, for example, forms the structural support for the oral disc, and the pericardial cartilage surrounds the heart of the lamprey through connection with the posterior region of the branchial basket (Fig. 1). Since the earliest observations of lamprey skeletal anatomy, it was long believed that lamprey cartilage was a hyaline cartilage, similar to that found in birds and mammals. However, close inspection by Wright et al. (1983, 1988) demonstrated that the cartilaginous elements of the sea lamprey are not hyaline cartilage but a new form of vertebrate cartilage. While the major fibrous element of mammalian and most non-mammalian cartilages is collagen, the extracellular matrix (ECM) of lamprey cartilages consists of a dense network of randomly arranged, branched, noncollagenous matrix fibrils (Wright and Youson, 1983; Wright et al., 1988). The major morphological features distinguishing the annular and pericardial cartilages include the more cellular nature of the pericardial cartilage and the more limited amount of matrix fibrils in the ECM of pericardial cartilage compared with the annular cartilage (Wright et al., 1988).

Biochemical characterizations have greatly enhanced our morphological understanding of lamprey cartilages. The resistance of annular cartilage to CNBr and NaOH digestion confirmed that the major structural protein of lamprey cartilages is not composed of collagen. Instead, a unique insoluble matrix protein, named lamprin, was found to constitute 44–51% of the dry mass of the annular cartilage (Wright et al., 1983; Robson et al., 1993). In the case of lamprey pericardial cartilage, amino acid composition analysis indicates significantly higher levels of hydroxyproline compared with annular cartilage (Robson et al., 1997). Morphological, biochemical and molecular biological analysis has demonstrated that the major matrix protein(s) of pericardial cartilage is not lamprin but yet another noncollagenous, elastin-like protein, despite it also being resistant to CNBr/NaOH digestion (Wright et al., 2001).

Taken together, previously established research and recent

biochemical studies indicate that the skeleton of the sea lamprey consists of a family of related, but non-identical, cartilages characterized by non-collagenous, elastin-like matrix proteins. Currently, we know nothing of the innate mechanical properties of lamprey cartilages nor of how their mechanical properties compare with those of mammalian cartilages. Consequently, the lamprey skeleton presents itself as a unique model from which we may broaden the current understanding of cartilage structure–function behavior. In conducting this investigation, we addressed the following questions: (1) do lamprey annular and pericardial cartilages exhibit a viscoelastic response to static mechanical loading; (2) do lamprey annular and pericardial cartilages demonstrate different equilibrium mechanical stiffnesses; (3) do adult lamprey cartilages stiffen with age and (4) do lamprey annular and pericardial cartilages differ from mammalian cartilages in their equilibrium mechanical stiffness? To answer these questions, we employed a series of equilibrium mechanical tests and morphological characterizations on two lamprey cartilages and one non-hyaline mammalian cartilage.

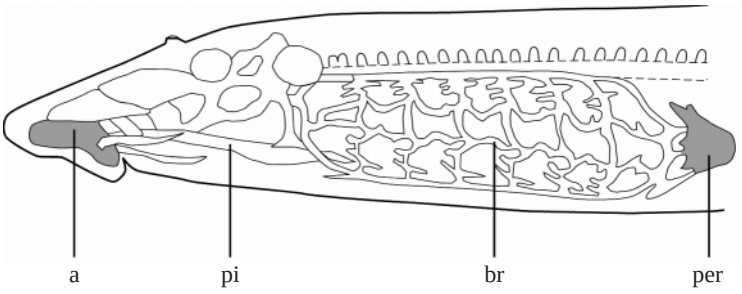

Fig. 1. Schematic diagram detailing several skeletal elements of the adult sea lamprey *Petromyzon marinus*. Annular cartilage (a), piston cartilage (pi), branchial cartilage (br), pericardial cartilage (per).

Materials and methods

Animals

Adult sea lamprey (*Petromyzon marinus* L.) were collected during upstream migration (early June 2000) at the LaHave River fish ladder in New Germany, Nova Scotia. After collection, lamprey were placed in two 10±2°C circular aquaria with aerated, recirculating freshwater (pH 7.4–7.5) and housed in a storage facility with low levels of ambient light. Annular and pericardial cartilage samples were harvested from 14 animals within 24 h of capture (young adults in early senescence), placed in lamprey Ringer's solution (Rovainen, 1973) and stored at –80°C. Ten animals were kept alive in the aforementioned conditions for a further 4 months (aged adults in late senescence) before annular and pericardial cartilage isolation. In all cases, cartilage specimen isolation was conducted after animals were anesthetized in a 0.05% solution of tricaine methanesulfonate (MS-222) and decapitated with a quick incision in front of the anterior-most gill slit. In total, two lamprey sample batches were used for experimentation: frozen young adult (N=14) and frozen aged adult (N=10). Freezing was found to have no effect on the morphological or mechanical properties of our studied cartilages (H.-W. Courtland, G. M. Wright, R. G. Root and M. E. DeMont, unpublished data). In addition to lamprey, several experiments were conducted on auricular (ear) cartilages harvested from four mature dairy cows (5–7 years old). Fresh bovine ears were obtained from the Antigonish, NS abattoir and, within 2 h, the skin and musculature were removed. Isolated auricular cartilages (with intact perichondria) were stored in lactated Ringer's solution (adapted from Quinn et al., 1982) at 10°C (changed daily) until the day of testing. Storage of auricular cartilage samples in this manner was less than one week.

Morphology and histochemistry

Water content was determined for young adult annular (N=8), young adult pericardial (N=8), aged annular (N=8), aged pericardial (N=5) and bovine auricular (N=8) cartilages. First, cartilage samples were thawed and cut as if for mechanical testing. Specimens were then equilibrated in lamprey or lactated Ringer's solution for 20 min, lightly blotted with Kimwipe® tissue paper and weighed on an analytical balance (accuracy 0.001 g). Finally, samples were dried in an oven at 80°C for 48 h. The wet mass minus the dry mass yielded the water content of the cartilage.

Annular (5 young and 5 aged each) and pericardial (5 young and 5 aged each) cartilage samples were taken from each of the two lamprey sample batches (before and after testing) in order to examine tissue morphology. Four bovine auricular cartilage samples were also taken from four separate animals for morphological analysis. Cartilage samples were fixed in either 80% ethanol for assessment of calcium deposition (Presnell and Schreibman, 1997) or 10% neutral buffered formalin to assess any disruption of tissue morphology resulting from the mechanical tests. All fixed tissues were then dehydrated through an ascending ethanol series, cleared in xylene and embedded in paraffin. Sections, 5–6 μm thick, were cut and mounted on glass slides previously coated with a 2% silane–acetone solution. For calcium assessment, the sections were stained using alizarin red S and alizarin red S after a 0.5 mol l^{-1} EDTA soak. Sections of formalin-fixed bovine muscle (calf skeletal muscle) containing a calcified lesion (white muscle disease) served as positive controls for these histochemical stains, and replicate sections treated with 0.5 mol l^{-1} EDTA prior to staining served as negative controls. Sections of the formalin-fixed and ethanol-fixed lamprey and bovine cartilages were also stained according to Harris' hematoxylin and eosin procedure (Prophet et al., 1992). Measurements of tissue structures at the light microscopic level were made using a calibrated ocular scale.

Isolated annular (aged; N=5), pericardial (aged; N=5), and bovine auricular cartilages (N=2) were prepared for high-resolution light microscopy and transmission electron microscopical analysis. Individual cartilage pieces were fixed in 2% glutaraldehyde in 0.1 mol l^{-1} phosphate buffer, pH

7.3–7.5 for 24 h at 4°C and post fixed (1% OsO_4 for 1 h at room temperature). Samples were then washed (0.1 mol l^{-1} phosphate buffer), dehydrated through an ethanol series and embedded in Spurr's resin. Thick sections (1 μm) were cut and stained with 1% toluidine blue in 1% sodium borate solution. Ultrathin sections (85–100 nm) were stained with uranyl acetate and Sato's lead stain before being examined using Hitachi H-600 and H-7500 electron microscopes operated at 75 kV and 80 kV, respectively.

Stress-relaxation equipment and sample preparation

Stress-relaxation experiments were conducted using a custom-built uniaxial lever system (Fig. 2) that accommodated two sets of adjustable, custom-engineered gripping devices. For tensile experiments, two stainless steel clamps with beveled ridges and metal spikes were created to hold cartilage samples firmly at both ends. Once clamped, the cartilage was trimmed to match the size of the clamp heads, gripping approximately 18 mm^2 of cartilage. Between the clamps, specimens were trimmed to yield a thin gauge region with relatively constant dimensions. For compression experiments, cartilage samples were held between two smooth, impermeable stainless steel plates. Clamped specimens were encased in a transparent bathing chamber filled with the appropriate Ringer's solution. Bovine cartilage runs were performed at room temperature (27±3°C), while lamprey cartilage runs were performed at 10±2°C. Before each experiment, the height of the top clamp/plate was adjusted to the position where the sample was just straight. In this position, the cartilage experienced negligible strain and an initial tare load of 0.1–0.2 mV (0.003–0.006 N). This initial 'pre-stress' was applied to ensure total contact over the specimen surface and to minimize the effects of surface irregularities.

Analysis of cartilage sample dimensions was made possible through the use of a CCD high-resolution video camera (Sanyo, Inc., Concord, ON, Canada; 2× magnification), which was manually positioned to take separate images from the front (length, width) and side (thickness) of each sample. For all acquired images, the camera was oriented 20 mm from the bathing chamber and perpendicular to the sample's axis of loading (Fig. 2). The length, width and thickness of each specimen were measured at five equally spaced positions along each dimension. Measurements of specimen length, width and thickness were manually computed using standard pixel analysis tools in LabView® (v.5.0, National Instruments, Inc., Austin, TX, USA). Using a variety of calibration objects, the measurement accuracy of this photo-digitizing method was estimated to be within 4%. All samples of a given cartilage type were of uniform shape and similar in size (Table 1).

Table 1. *Mean resting length, width and thickness (mm) of gauge regions (± S.D.) for lamprey pericardial and annular cartilages and bovine cartilages tested in tension and compression*

	Pericardial tension	Annular compression	Bovine tension	Bovine compression
Length	7.2±1.0	3.9±0.4	9.5±3.7	3.7±0.4
Width	3.7±0.5	4.3±0.8	5.6±0.4	4.4±0.1
Thickness	1.0±0.2	3.2±0.5	1.7±0.8	3.9±0.2

Stress-relaxation experiments

The experiments conducted were dependent upon the morphology of the cartilage tissues and the ability of the testing machinery to clamp specimens adequately. With these considerations in mind, uniaxial tensile tests were performed on lamprey pericardial cartilage samples (*with* attached perichondria) sectioned from the animal's dorsal plane and oriented laterally around the tissue's caudal apex (Fig. 3A). In this fashion, the loading axis was parallel to the plane of the perichondria. Uniaxial compressive tests were performed on dorso-ventrally oriented samples (without perichondria) taken from the anterior-most portion of the lamprey annular cartilage ring (Fig. 3B). For bovine auricular cartilage, uniaxial tensile tests were performed on lengthwise samples (distal-proximal to the head) without perichondria, and uniaxial compressive tests were performed on dorso-ventrally oriented samples without perichondria (Fig. 3C,D).

All stress-relaxation experiments consisted of unconfined uniaxial deformations enabling the quantification of equilibrium stresses after fluid loss and shape changes along the tissue's longitudinal and lateral dimensions. Prior to each stress-relaxation run, cartilage samples were allowed to equilibrate for 20–30 min in the bathing chamber. Then, a multifunction synthesizer (8904A DC-600 MHz, Hewlett Packard, Inc., Palo Alto, CA, USA) directed the motorized lever (Model 300 Servo System Lever; Cambridge Technology, Inc., Watertown, MA, USA) to impose near instantaneous (<1 s) fixed deformations (fixed strains) on the cartilage samples. Each sample's resistance to deformation was interpreted as a voltage output, which was read by a digitizing oscilloscope (54501A 100MHz;

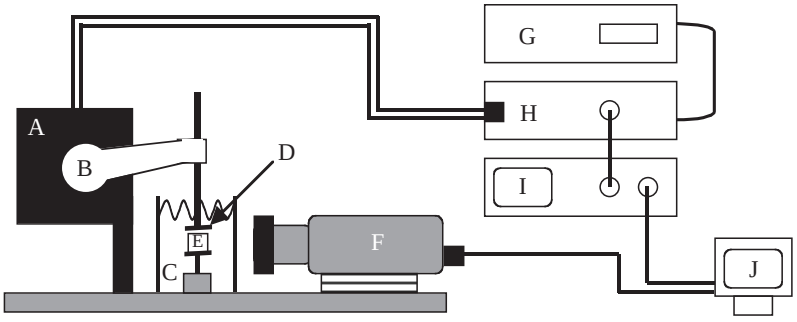

Fig. 2. Schematic diagram of the custom-built uniaxial lever system and associated instrument interfaces. Servo motor (A), lever arm (B), bathing chamber (C), cartilage plate/clamp (D), annular cartilage sample (E), video camera (F), multifunction synthesizer (G), Servo motor control console (H), digitizing oscilloscope (I), computer (J).

Hewlett Packard, Inc.). LabView® (v.5.0) was used to automate the entire process, storing voltage data every 4 s until equilibrium. Equilibrium was initially determined by visual inspection and subsequently quantified by calculation of the time where $\Delta V/\Delta t=0$ (V is voltage, t is time) for ±5 min. The resulting equilibrium voltage required to maintain the applied strain deformation in tension (or compression) was recorded and this process repeated 3–5 times, allowing recovery of the cartilage between each trial, defined as each sample's return to its initial shape and initial pre-stress load.

Stress-strain analysis

According to isolation, the dominant dimension was considered the length for each cartilage sample, and tensile/compressive deformations were imposed along this longitudinal axis. The resting length (L_0) and resting stress (σ_0) of each cartilage sample's gauge region were measured prior to testing. In addition, the width and thickness of each gauge region were measured at five equidistant points along the length of the sample after each instance of deformation. From these values, the mean thickness (*th*) and width (*w*) were calculated, the product of which was the mean cross-sectional area (A) for the cartilage sample. After deformation, the extension or compression of each sample ΔL was calculated using:

$$\Delta L = | L - L_0 | , \quad (1)$$

and the longitudinal, applied strain (ε) experienced by the sample was then defined as:

$$\varepsilon = (\Delta L) / L_0 . \quad (2)$$

Strain increments ranged from 1.0% to 16.75% and 4.3% to 21.4% for tensile and compressive experiments, respectively. For stress determination, the equilibrium voltage was subtracted from its respective pre-load voltage and then converted to an equilibrium force ($\mathbf{F}_e$) using calibrated weights. Each $\mathbf{F}_e$ was then converted to equilibrium stress (σ_e) using:

$$\sigma_e = \mathbf{F}_e / A . \quad (3)$$

The equilibrium modulus, or equilibrium stiffness (E), was calculated as the slope of each linearly regressed $\sigma_e - \varepsilon$ plot (stress-strain curve):

$$E = \Delta\sigma_e / \Delta\varepsilon . \quad (4)$$

Statistical analysis

Determination of cartilage modulus values was performed using a standard least-squares regression fit to our experimentally determined stress-strain data, and in this manner all stress-strain plots yielded regression fits with r^2 values of ≥0.80. To evaluate differences in mean modulus values and mean water contents of different cartilages, single-factor analysis of variance (ANOVA) was performed after confirming the normality of residuals and using Minitab® statistical software (v.12, Minitab, Inc., State College, PA, USA). If an ANOVA indicated the presence of a significant difference, Tukey multiple comparison tests were performed to determine specific mean differences. The abovementioned statistical tests were all performed with an upper limit of significance at P=0.05.

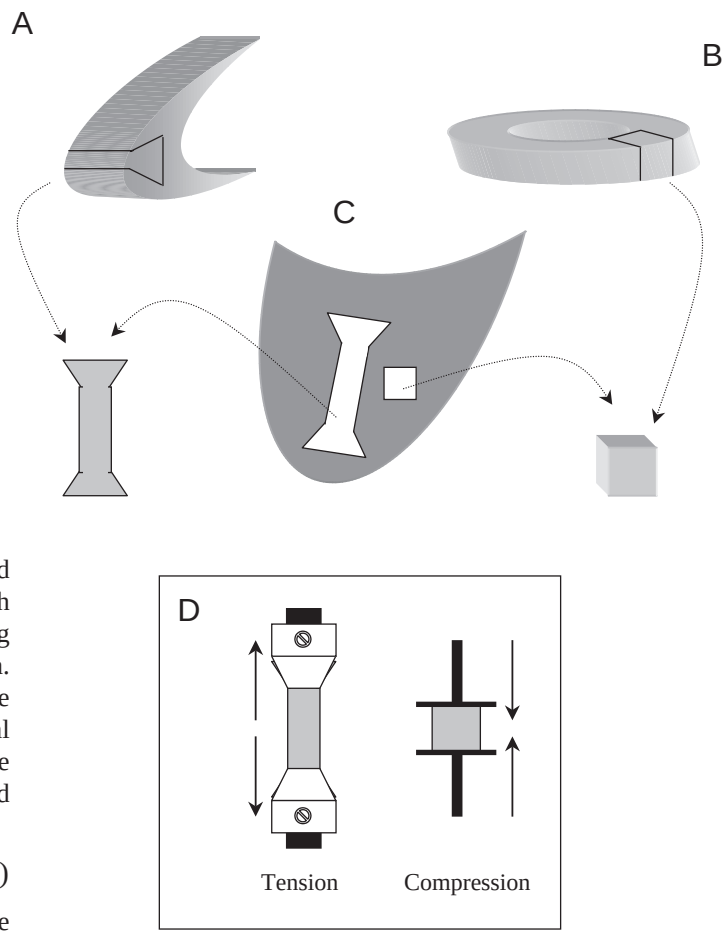

Fig. 3. Schematic diagram illustrating the orientation of cartilage samples during isolation and experimental loading. Samples from lamprey pericardial cartilage (A) were taken across the posterior portion of the 'bowl-like' tissue (note that only part of the sample appears in the three-dimensional view). Lamprey annular cartilage samples (B) were cubes taken from the anterior portion of the annular ring. Bovine auricular cartilage samples (C) were taken for both tensile and compressive tests (D).

Results

Cartilage morphology

Qualitative macroscopic examination of isolated cartilage samples revealed that young annular cartilage (with or without perichondria) exhibited a rather 'hard' consistency whether part of the intact ring or as separate pieces. However, thin slices of annular cartilage (≤2.0 mm thick, no perichondria) were best described as 'brittle' with little resistance to bending or stretching deformations. In contrast to the annular cartilage,

young pericardial cartilage was best described as a 'soft' tissue that easily permitted deformation. However, upon removal of both collagenous perichondria, the remaining cartilage was found to be substantially weaker with virtually no resistance to deformation. Also of note were apparent differences between young pericardial cartilage perichondria. When separated from the underlying cartilage, the outer perichondrium (i.e. that exposed to the lamprey body cavity) gave great resistance, often tearing the cartilage as it was removed. By contrast, the inner perichondrium (i.e. that exposed to the pericardial cavity) gave little resistance to separation. These qualitative descriptions of young annular and pericardial cartilages also held true for aged annular and pericardial cartilages. However, it was noted that, although still flexible, the intact aged pericardial cartilage offered greater resistance to bending deformations before an eventual 'snapping' of the cartilage/perichondria structure. No unusual observations were made from bovine auricular cartilage, although the consistency of the isolated cartilage (with or without perichondria) was best described as 'hard', similar to the lamprey annular cartilage, but, unlike the annular cartilage, it was found to retain this consistency even when sliced thin (i.e. it was not brittle).

While extensive light microscopical analyses of lamprey annular and pericardial cartilages have been reported (Wright and Youson, 1983; Wright et al., 1988; Robson et al., 1997), several previously unpublished structural features were observed during this investigation. The perichondria of the pericardial cartilage (young and aged) give boundaries, as the cartilage forms the pericardium enclosing the heart and supports it within the body cavity (Fig. 1). The outer perichondrium (exposed to the body cavity) was found to be thin (≈20–40 μm) with densely packed collagen fibers. The inner perichondrium (lining the pericardial cavity) is 2–4 times as thick (≈80–120 μm) as the outer perichondrium, largely due to the presence of what appears to be a looser arrangement of collagen fibers containing large adipose cells and blood vessels (Fig. 4A). The central positioning of these cells and blood vessels allows for a delineation of the inner perichondrium into two layers, one contacting the cartilage and the other contacting the pericardial cavity. In annular cartilage (young or aged), there is no obvious boundary for perichondria. Instead, the perichondria tend to blend with a variety of adjacent connecting tissues (Fig. 4B). Depending on location, the perichondria can be seen merging with overlying layers of muscle and even adipose tissue. The dense collagenous perichondria of bovine auricular cartilage were similar to that of the annular cartilage in that they blend with adjacent connective tissues (Fig. 4C).

Hematoxylin/eosin staining gave identical results for young adult and aged lamprey cartilages, although staining differences between the two lamprey cartilage types were observed. 'Hard' annular cartilage ECM and perichondria were found to stain bright pink/red (acidophilic) with eosin (Fig. 4B). Bovine auricular cartilage ECMs and perichondria also stained pink/red with eosin (Fig. 4C) although, in the case of the ECM, eosin staining was mainly associated with elastic fibers while the remainder of the ECM was found to stain a light gray/blue (weakly basophilic). The 'soft' pericardial cartilage ECM demonstrated a staining pattern opposite to that of annular cartilage, as evidenced by blue staining (basophilic) with hematoxylin, but the outer and inner perichondria stained pink/red (Fig. 4A). A slight difference in subperichondrial ECM concentration was noted between the outer and inner perichondria of lamprey pericardial cartilages. Specifically, ECM adjacent to the outer perichondrium appeared to form thicker seams between smaller chondrocytes than in the inner perichondrium, where thin seams of ECM surrounded large chondrocytes.

Alizarin red S stains were used for histological assessment of calcium deposition at three pH levels. The positive control gave light, moderate and high intensity red staining within a known calcified lesion for pH levels of 9, 6.4 and 4.2, respectively. Alizarin red staining at a pH of 4.2 gave the most vibrant stain colorations in cartilage samples. The ECM and cellular matrix (CM) regions of all pericardial cartilages exhibited a strong orange/red tint, while all annular cartilage ECMs gave a strong yellow coloration. Perichondria of all cartilages demonstrated a proportional increase in color intensity (as compared with staining of the pure cartilage tissue) and appeared dark red and/or orange. Replicate sections of young and aged lamprey annular and pericardial cartilage pre-treated with 0.5 mol l^{-1} EDTA were all found to stain a pale red with alizarin red pH 4.2. Thus, the high intensity of staining, particularly in the perichondria of pericardial and annular cartilages, was not apparent for staining after pre-treatment with EDTA. Bovine auricular cartilage resembled the EDTA-pre-treated negative control by staining pale red with alizarin red pH 4.2.

Analysis of aged and young cartilage ultrastructure gave no evidence of mineralization. The only notable difference between aged and young lamprey cartilages was an apparent degeneration of aged pericardial cartilage outer perichondria, which were found lacking their epithelial cell layer. The epithelial cell layers of inner perichondria appeared intact in both young and aged lamprey pericardial cartilages. Ultrastructural examination of lamprey cartilages and bovine auricular cartilages showed no other differences from previous publications on these tissues (Wright and Youson, 1983; Serafini-Fracassini and Smith, 1974b), confirming that our mechanical tests did not alter the structural integrity of the tissues.

Lamprey pericardial cartilage sections cut parallel to the plane of the perichondrium revealed that collagen fibers of both the inner and outer perichondria were not aligned along a specific line of orientation but existed in a staggered array (Fig. 5). Within this array, collagen fibers were rarely oriented parallel to each other. Instead, fibers typically demonstrated inter-fiber angles ranging from 30° to 90°. There were no noticeable differences in perichondrial fiber orientation between inner and outer perichondria or between young and aged cartilages.

Both young and aged lamprey annular cartilages were found

to contain canal-like structures at all tissue depths (Fig. 6). These canals ranged from 80 μm to 600 μm in diameter, and the cartilage immediately surrounding the canals consisted of dense ECM with many flattened chondrocytes. The canals typically contained loose connective tissue with appreciable quantities of an amorphous ground substance, which contained randomly arranged, widely dispersed fibers and blood vessels. Microscopical examination of annular cartilage sections revealed that canals were sufficiently abundant throughout the tissue to render the testing of regions without canals impossible. No canal structures were observed in lamprey pericardial (young or aged) cartilages or bovine auricular cartilages.

Viscoelasticity

Characteristic water contents (% wet mass) of lamprey and bovine cartilages are listed in Table 2. All cartilages were found to possess a water content constituting >60% of the cartilage's wet mass. The mean water content for bovine auricular cartilage was found to be significantly lower than

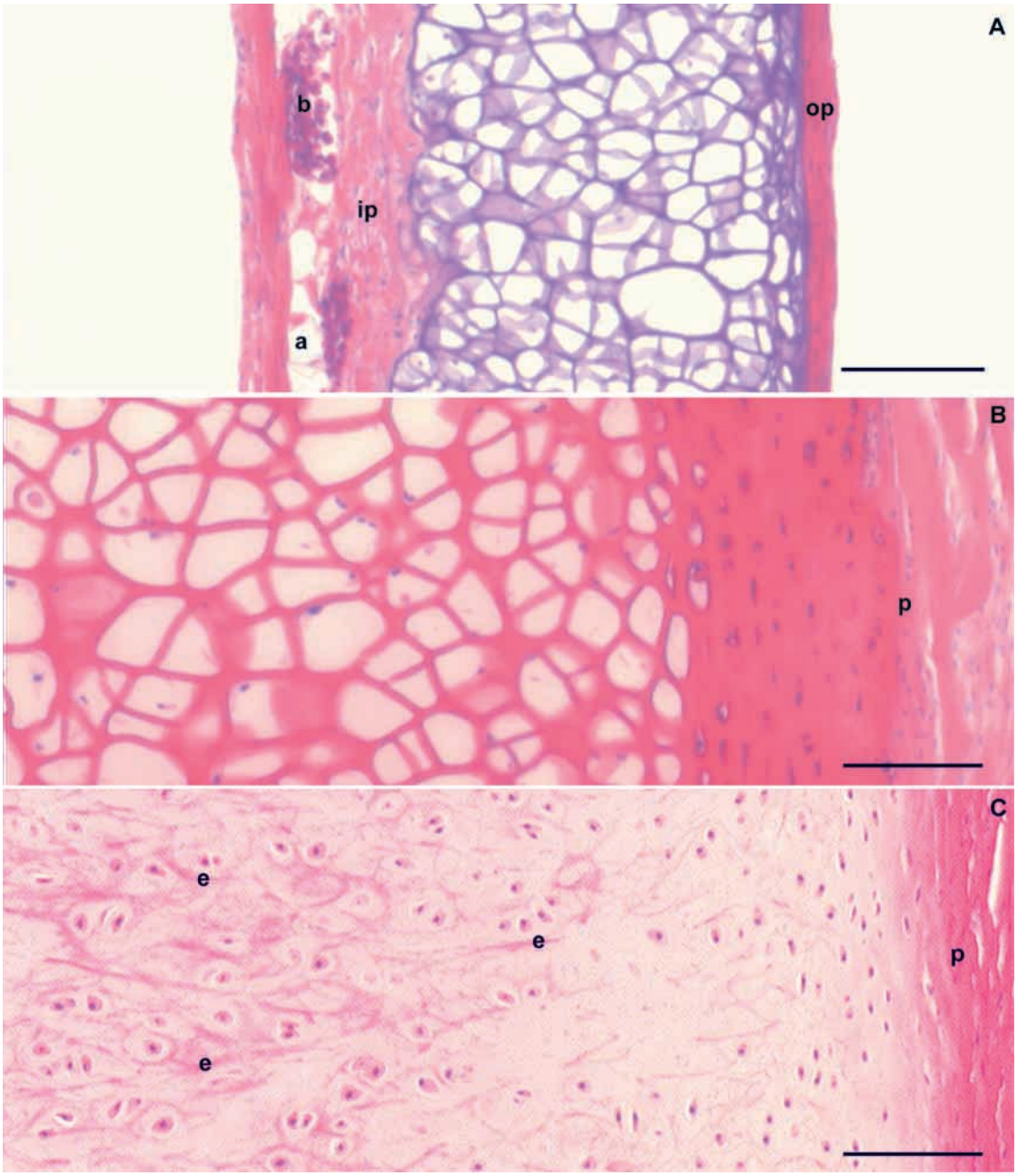

Fig. 4. Representative hematoxylin and eosin staining of lamprey and bovine cartilages. (A) Lamprey pericardial cartilage. (B) Lamprey annular cartilage. (C) Bovine auricular cartilage. Outer perichondrium (op), perichondrium (p), inner perichondrium (ip), blood vessels (b), adipose cells (a), elastic fibers (e). Scale bars, 100 μm.

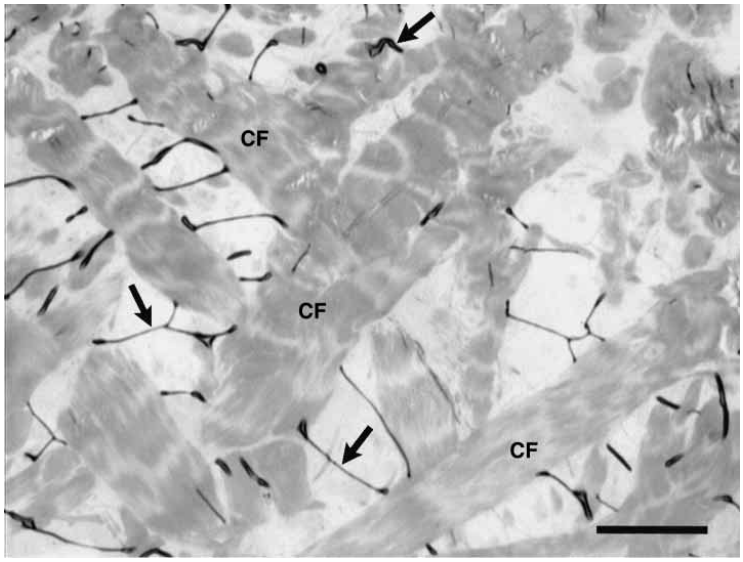

Fig. 5. 1-μm-thick toluidine blue-stained horizontal resin section of lamprey pericardial cartilage illustrating the non-parallel arrangement of collagen fibers (CF) in the outer perichondrium. Arrows indicate small folds in the section. Scale bar, 40 μm.

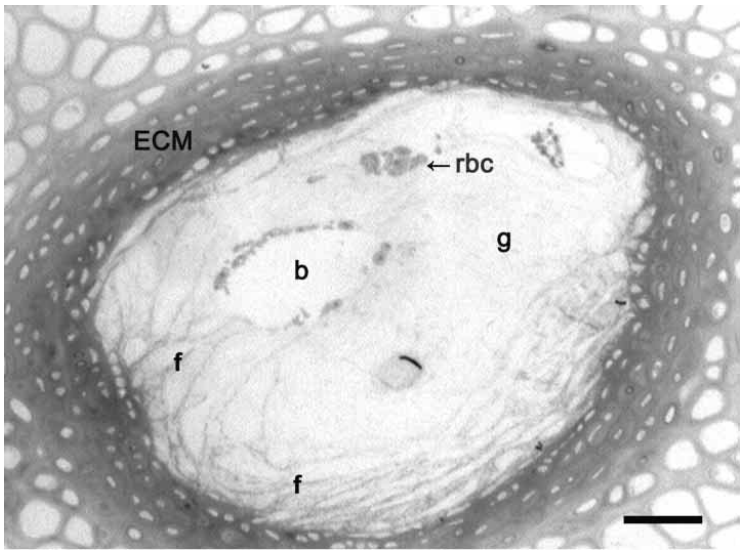

Fig. 6. 1-μm-thick toluidine blue-stained lateral resin section of lamprey annular cartilage showing a typical cartilage canal. Noncollagenous extracellular matrix (ECM), red blood cells (rbc), blood vessel (b), ground substance (g), collagen fibers (f). Scale bar, 70 μm.

those of lamprey annular and pericardial cartilage (young adult and aged), although this is probably not physically significant. Lamprey annular and pericardial cartilages gave mean water contents that were statistically indistinguishable and there were also no differences in mean water content between young and aged samples of lamprey annular and pericardial cartilage.

All tested cartilages demonstrated a time-dependent stress response to loading (Fig. 7). That is, there was a characteristic stress-decay behavior and characteristic length of time (equilibrium time, t_e) required for cartilage samples to reach σ_e. Bovine auricular cartilage, gave t_e that were identical for both tensile and compressive loading. There were, however, noticeable differences in t_e among the different cartilage tissues (Table 2). Both young and aged lamprey annular and pericardial cartilages required a period of at least 120 min to reach equilibrium after the initial strain was applied. Bovine auricular cartilage differed in its t_e, requiring only 30 min to reach equilibrium. After reaching t_e, all cartilage samples exhibited complete recovery upon removal of the imposed strain deformations as demonstrated by 100% recovery to both their initial shape and σ_0. Still, variations in recovery time (t_r) were found (Table 2) and, although semi-quantitative, they afford clear distinctions. Lamprey pericardial cartilage (both young and aged) required the shortest t_r of all the cartilages (<0.5 min). Bovine auricular (tension and compression) and lamprey annular (both young and aged) cartilages gave substantially longer t_r values of 30 min and 120 min, respectively. Note that t_r is identical to t_e for these two cartilages. However, while bovine auricular cartilage required 30 min to return to its initial σ_0, it required <0.5 min to recover to its initial shape; upon removal of the deformation, the recovery of σ_0 lagged behind the near instantaneous recovery of shape.

Preliminary work on modeling the viscoelastic properties of lamprey and bovine cartilages has been previously set forth (Courtland, 2001). In accordance with this approach, all cartilages studied in this investigation exhibited non-exponential (non-linear) decay behavior as supported by two observations. First,

Table 2. *Mean water contents (± S.D.), approximate equilibrium (t_e) and recovery (t_r) times for lamprey and bovine cartilages*

	Young adult annular	Young adult pericardial	Aged adult annular	Aged adult pericardial	Bovine auricular	Auricular tension	Auricular compression
% Water	76.5±4.5[a]	77.4±4.2[a]	77.7±1.5[a]	81.4±2.8[a]	70.0±2.6	N/A	N/A
t_e	120 min	120 min	120 min	120 min	N/A	30 min	30 min
t_r	120 min	<0.5 min	120 min	<0.5 min	N/A	30 min	30 min

N/A, not applicable.

Water content was calculated as a percentage of the cartilage wet mass. Statistically indistinguishable water contents (P>0.05) are indicated by the presence of a shared superscript ‘a’.

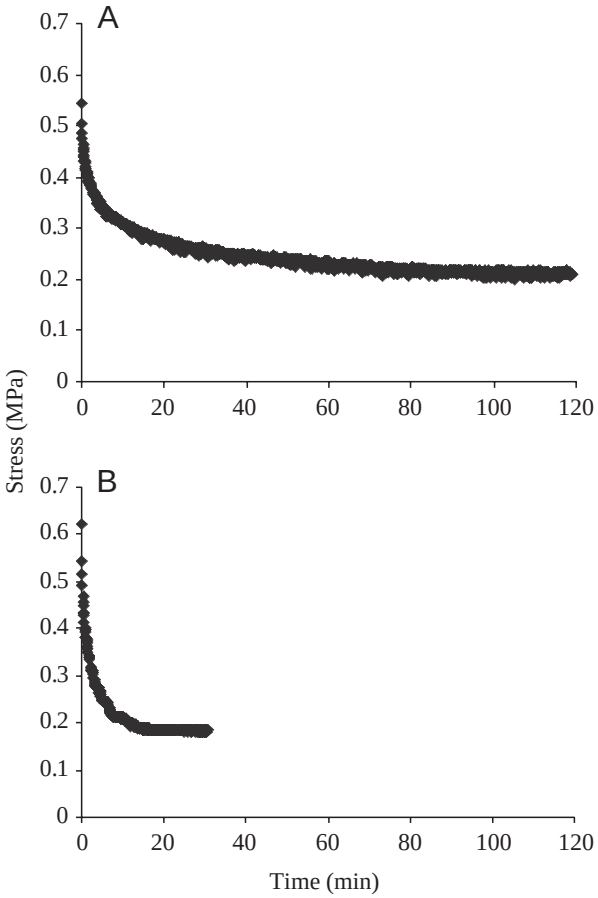

Fig. 7. Characteristic stress-relaxation curves for cartilages. (A) Aged annular cartilage sample under an 8.5% compressive strain. (B) Bovine auricular cartilage under a 17.5% compressive strain.

there were demonstrable nonlinear variations of the centered difference approximation to the decay rate $(\sigma_{n-1}-\sigma_{n+1})/(t_{n+1}-t_{n+1})$ *versus* σ_n for these cartilages. Second, using

$$\frac{d\sigma}{dt} = -k(\sigma - \sigma_e)^p \qquad (5)$$

as a model to fit the stress-relaxation (in which σ_e is the equilibrium stress, k is the proportionality constant between relaxation rate and a power of the deviation from equilibrium, and *p* is that power), both lamprey and bovine data gave values of the parameter *p* that were always greater than one.

Equilibrium stiffness

In all cartilages, the stress-strain data were best described with linear regressions (there was no indication of curvilinear behavior through the tested range of strains; Fig. 8). Mean equilibrium moduli, or equilibrium stiffnesses (*E*), are listed in Table 3 and ranged from 0.71 MPa to 4.85 MPa. An ANOVA indicated the presence of at least one significant difference among the reported mean *E*, and a series of Tukey comparison tests yielded a total of nine significant differences among them.

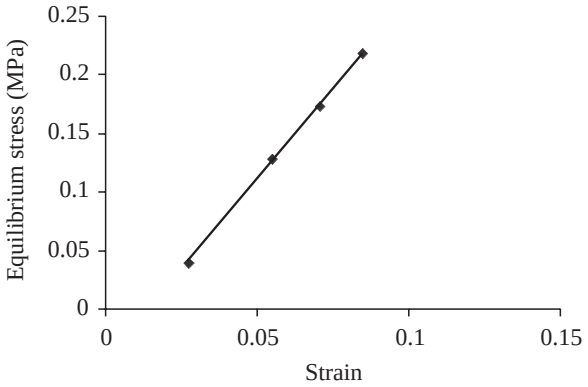

Fig. 8. Characteristic stress-strain curve for lamprey cartilage. Data shown are from an aged lamprey annular cartilage sample. The linear regression equation for this curve is $y=3.0898x-0.0446$, $r^2=0.99$.

Table 3. *Mean equilibrium moduli (*E*) ± S.D. for lamprey and bovine cartilages*

Cartilage	*N*	Mean *E* (MPa)
Young adult annular	8	0.71 ± 0.30^{a}
Aged adult annular	6	$1.18\pm0.70^{a,b}$
Young adult pericardial	11	2.87 ± 0.56^{c}
Aged adult pericardial	5	4.85 ± 1.46^{e}
Bovine (tension)	3	$1.94\pm1.40^{a,b,c,d}$
Bovine (compression)	4	$1.29\pm0.28^{a,b,c,d}$

Where two means share the same superscript letter, they are statistically identical ($P>0.05$).

As can be seen from Table 3, there are clear differences in mean *E* between lamprey cartilages. Young pericardial cartilage possessed a larger mean *E* than young annular cartilage. In addition, aged pericardial cartilages demonstrated a significantly larger mean *E* in comparison with all annular cartilages. Aged lamprey pericardial cartilage also had a larger mean *E* than that of young pericardial cartilages. However, comparison of aged *versus* young annular cartilage demonstrated no significant difference in mean *E*. There was no difference between the mean *E* values of bovine auricular cartilages tested in tension and compression. In addition, both young and aged annular cartilages gave mean *E* that were not significantly different to the tensile and compressive mean *E* of bovine auricular cartilages. The mean *E* of young adult lamprey pericardial cartilages was also not significantly different to either of the bovine mean *E*; however, aged pericardial cartilage possessed a mean *E* significantly larger than that of either bovine group.

Discussion

Morphology and viscoelasticity

Bovine auricular cartilage and all lamprey cartilages were found to contain substantial quantities of water (≥70%), which afforded these tissues significant viscoelastic properties. It is

important to note that t_e (and t_r) may, for certain cartilages, be dependent upon the size of the loaded sample (Mow et al., 1980). However, this volume dependence has not been thoroughly addressed in the literature and, as a result, these parameters are discussed here irrespective of their corresponding sample volumes.

The t_e of lamprey annular cartilage was approximately 120 min. This is the longest relaxation time reported for any vertebrate cartilage; the typical t_e for human and bovine articular cartilage is 15 min (Akizuki et al., 1986; Schmidt et al., 1990). Such a long t_e for lamprey annular cartilage is suggestive of an extremely low permeability for this tissue, and there are three factors that may contribute significantly to this behavior: canal structures, ECM proteoglycans (PGs) and ECM fibrils. The presence of canals is not unique to lamprey annular cartilage but is a feature common to 'thick' mammalian cartilages such as rib and epiphyseal growth cartilage (Shingleton et al., 1997; Craatz et al., 1999). In lamprey annular cartilage, the combination of the canal walls and the surrounding dense ECM region may serve to decrease permeability of the cartilage by creating a surface around which drag forces arise. In terms of PGs, lamprey annular cartilage contains mostly *N*-acetyl galactosamine-containing glycosaminoglycans (GAGs; Wright et al., 1983). Since the majority of characterized *N*-acetyl galactosamine-containing GAGs are found in chondroitin sulphate, keratin sulphate and hyaluronate PGs (Serafini-Fracassini and Smith, 1974a), this would suggest that the PGs of lamprey annular cartilage are similar to the low conductivity PGs of mammalian articular cartilages in that they too incorporate a substantial number of alternating GAG β1,4 and β1,3 linkages. This would help to explain the low permeability of lamprey annular cartilage as a function of increased flow resistance around PG GAG side chains (Comper and Zamparo, 1990; Comper and Lyons, 1993). Still, one must remember that lamprey annular cartilage has a t_e that is twice that of rabbit articular cartilage (Mow et al., 1989). As an additional factor, we propose a functional significance for the lamprin-based ECM fibrils that, at the ultrastructural level, exist as a highly branched three-dimensional network (Wright et al., 1983; Wright and Youson, 1983) quite unlike the non-branched arrangement of collagen fibrils in mammalian articular cartilages (see Oloyede and Broom, 1996 for a review). The effect of branched fibrils may be to permit a significant surface area for hindering the rate of fluid flow from annular cartilage. This would give rise to a lower permeability for this tissue and explain the longer t_e as compared with mammalian cartilages. The t_r for annular cartilage was also approximately 120 min, suggesting that the recovery process, in which extruded water is drawn back into the tissue, encounters the same drag-induced forces as were experienced during stress-relaxation, despite the influence of Donnan osmotic forces that would encourage fluid flow back into the cartilage. Equal resistance to extrusion and imbibition of water is in line with drag-induced low permeability possibly arising from canal structures, low conductivity PGs and branched ECM fibrils.

When considering the t_e of lamprey pericardial cartilage, which was also found to be approximately 120 min, the aforementioned contributions of PGs and ECM fibrils to reduced permeability may be valid. However, the extent of their contributions is less clear due to a lack of knowledge regarding the chemistry of pericardial cartilage PGs and also due to the substantially reduced quantity of ECM fibrils. There is also reason to believe that other features, such as chondrocytes and adipose cells, may influence this tissue's viscoelastic properties. The chondrocytes of lamprey pericardial cartilage occupy a considerably larger volume fraction than those of the annular cartilage (compare Fig. 4A and Fig. 4B) and, as a result, they account for most of the tissue's total volume. Since lamprey annular and pericardial cartilages were found to have identical water contents and most of the pericardial volume exists as chondrocytes, it can be assumed that most of the bound water in pericardial cartilage is intracellular. Work by Freeman et al. (1994) demonstrated that chondrocytes impart a substantial viscoelastic effect to agarose gels that they were cultured in, and other research has shown that chondrocytes exhibit viscoelastic behavior common even to whole cartilage (for a review, see Guilak, 2000). It is therefore conceivable that the viscoelastic behavior of pericardial cartilage is largely a function of chondrocyte viscoelasticity. Given that the t_e for pericardial cartilage is 120 min, it seems likely that this effect would result from chondrocyte fluid exudation. Adipose cells may also contribute to the viscoelastic characteristics of lamprey pericardial cartilage, but further investigation is required.

If viscoelastic effects (e.g. drag and fluid redistribution) were truly the only determinants of lamprey pericardial cartilage's permeability, then a t_e of 120 min could not accommodate a t_r of $\ll$120 min. Yet, all pericardial cartilages recovered fully to their initial shape and σ_0 in <30 s. This phenomenon can best be explained as a result of testing the pericardial cartilages with their attached perichondria. The perichondria are composed mainly of collagen fibers (see Fig. 5). Since the tensile *E* for pericardial cartilages was two orders of magnitude smaller than that for pure collagen, stress-minimization *via* intrafibrillar contraction of collagen seems an unlikely determinant of pericardial cartilage's short t_r. A more likely explanation is the potential crosslinking of perichondrial collagen with the surrounding electron-dense elastic-like fibers (see Wright et al., 1988), which could permit tensile loading-induced fiber reorientation. If this were true, then release of the tensile load after equilibrium would permit a rapid minimization of this high-energy conformation, thereby explaining the observed small t_r. Regardless of the exact mechanism behind t_r<30 s, it is clear that the initial shape and σ_0 of pericardial cartilages are determined by the tissue's collagenous perichondria alone, and it follows that any t_r based on these parameters will not necessarily indicate the true recovery behavior of the tissue's CM and ECM. Thus, the t_r reported here for lamprey pericardial cartilages is best viewed as an *apparent* recovery time, one that is partially independent of and hides the tissue's true viscoelasticity.

Bovine auricular cartilage gave a t_e of 30 min for both tensile and compressive deformations. This is substantially shorter than the t_e of both lamprey annular and pericardial cartilages, suggesting that bovine auricular cartilage has a comparatively larger permeability. Possible explanations for this behavior are the presence of more PGs, a higher percentage of high-conductivity PGs and a less-connected arrangement of structural proteins in bovine auricular cartilage. The t_r of bovine auricular cartilage for both tension and compression was found to be identical to the t_e (approximately 30 min), suggesting a certain degree of structural homogeneity for this tissue. In addition, this suggests that in auricular cartilage, the σ_0 load is borne not by the elastic or collagenous structural fibers but by the cartilage's Donnan osmotic pressure, the recovery of which requires a time period equivalent to that of the stress-relaxation experiment (about 30 min). It must be noted, though, that auricular cartilage's recovery to its initial shape required a time substantially less than 30 min (<0.5 min) and this is probably due to recoil of elastic fibers and/or an overall reorientation of the fibrous network. We must then define the *true* t_r for bovine auricular cartilage as one indicated not by the recovery of shape alone but by the recovery of σ_0 *and* shape. Given the differential recovery of both lamprey pericardial and bovine auricular cartilages, it seems that assessing the *actual* recovery of loaded cartilages can be quite difficult.

The above discussion has suggested that lamprey cartilages have markedly lower hydraulic permeabilities than mammalian cartilages and, if so, this must be related to the mechanical function of these tissues. In lamprey pericardial cartilage, the role of low permeability is probably to prevent relaxation of the tissue during short intervals of loading. Since the cartilage is very thin and the majority of fluid originates from its chondrocytes and/or adipose cells, even a small relaxation of these components would decrease cartilage Donnan osmotic pressure and the cartilage as a whole would be less flexible and less resilient. That is, the pericardial cartilage would be virtually incapable of absorbing/releasing any expansion/recoil forces imparted to it by the heart and branchial basket. In lamprey annular cartilage, the low permeability is more likely to be a mechanism for the dissipation of energy over longer intervals of time (i.e. feeding). The highly branched lamprin fibril network probably affords a greater surface area (per fibril volume) over which forces are distributed, thus minimizing the load borne by individual fibrils and transferred through the aqueous phase of the ECM. It is important to note that while lamprey cartilages appear to differ from mammalian cartilages in their permeabilities, they each exhibit a non-linear stress-decay behavior that is also characteristic of mammalian articular cartilages (Mansour and Mow, 1976; for a review, see Maroudas, 1979).

Stiffnesses

For the intrinsic, static parameter *E*, charge effects are normally the major contributing factors in the ability of cartilage to resist compressive deformations. A list of compressive *E* can be found in Table 4 and from these it is clear that the compressive *E* of young adult lamprey annular cartilage is nearly identical to the compressive *E* reported for bovine articular cartilage (hyaline cartilage) as well as bovine meniscus (fibrocartilage). The reported *E* for lamprey annular cartilage is somewhat smaller than for human articular cartilage and bovine auricular cartilage but is nonetheless within one order of magnitude of both. Possible determinants of the similarities in compressive stiffness between lamprey annular cartilage and mammalian cartilages include the incorporation of similarly charged PGs and similar ionic contents. In addition, the lamprin ECM fibrils may contribute to the tissue's compressive stiffness through extensive fibril interactions (i.e. flow resistance).

Table 4. *Reported mean moduli (*E*) ± S.D. (when available) for various biological structures tested in compression*

Structure	Mean *E* (MPa)
Subchondral bone (human tibia)[1]	300–450
Human articular cartilage[2]	4.31±1.01 to 9.43±1.44
Bovine auricular cartilage[3]	1.29±0.28
Aged adult annular cartilage[3]	1.18±0.70
Bovine articular cartilage[4]	0.96±0.47
Bovine articular cartilage[5]	0.677±0.22
Young adult annular cartilage[3]	0.71±0.30
Bovine meniscus[6]	0.410±0.088

[1]Aitken et al. (1985); [2]Yao and Seedhom (1993); [3]present study; [4]Wong et al. (2000); [5]Jurvelin et al. (1997); [6]Proctor et al. (1989).
All moduli are equilibrium moduli except for subchondral bone.

When considering the ability of connective tissues to resist tensile forces, structural proteins are usually of fundamental importance. The fact that lamprey pericardial cartilage easily disintegrates in the absence of its perichondria suggests that the pure cartilage has a very low tensile *E* compared with the intact tissue with both perichondria attached. The ECM fibrils, scarce in comparison to the tissue's fraction of chondrocytes, must therefore play only a minor role in the tensile *E* of the cartilage. Consequently, in order to resist loads while at the same time preserving the viscoelastic properties of the tissue, the pericardial cartilage employs perichondrial layers composed of a dense network of collagen fibrils. This gives rise to a tensile *E* that is significantly larger than the compressive *E* of lamprey annular cartilage. A listing of reported tensile *E* can be found in Table 5 and shows that young adult lamprey pericardial cartilage is comparable with mammalian cartilages in its tensile *E* but clearly falls in the low end of reported cartilage *E*. Since research has also shown that the number of hydroxypyridinium cross-links within collagen fibrils directly influences the tensile *E* and strength of the intact cartilage (Schmidt et al., 1987), the relatively low volume fraction content of collagen fibers in the perichondria (Fig. 4A) and the non-parallel orientation of these fibers (Fig. 5) may be particularly relevant to the lower *E* of lamprey pericardial cartilage.

Table 5. *Reported mean equilibrium moduli (*E*) ± S.D. (when available) for various biological structures tested in tension*

Structure	Mean *E* (MPa)
Human tracheal cartilage[1]	1.8–15
Human articular cartilage[2]	1.0–15
Human tracheal cartilage[3]	5.4–11.1
Canine tracheal cartilage[4]	10.38±2.11
Young adult pericardial cartilage[5]	2.87±0.56
Aged adult pericardial cartilage[5]	4.85±1.46
Bovine auricular cartilage[5]	1.94±1.40
Elastin[6,7]	1.0

[1]Rains et al. (1992); [2]Akizuki et al. (1986); [3]Roberts et al. (1998); [4]Hamaide et al. (1998); [5]present study; [6]Dimery et al. (1985); [7]Vogel (1988).

The fact that both young pericardial and bovine auricular cartilages give comparable tensile *E* suggests that they may share common features. Indeed, both cartilages have a low density of collagen fibers/fibrils when compared with hyaline and fibrocartilages, and both contain ECM fibrils demonstrating biochemical similarities to elastin. Still, in pericardial cartilage, the collagen fibers are fairly well organized in the perichondria but are a small fraction of the total tissue volume. When compared with auricular cartilage, where collagen fibrils constitute up to 80% of the fibrous content (Stockwell, 1979) and are distributed throughout the tissue, the similarity in tensile *E* of these two cartilages is startling. Of course, with such a low sample size for bovine auricular cartilage, the mean *E* may not be truly representative of a population, but, assuming the similarity is real, lamprey pericardial cartilage may be circumventing a dearth of collagen by incorporating a select number of fibers at high density in critical regions (perichondria), by orienting fibers in an optimal way or by developing more-extensive fibril cross-links within fiber fibrils. Further biochemical analyses are necessary to validate these possibilities.

Similar to the classification reported here for lamprey, the cartilaginous elements of the hagfish have been characterized as either hard or soft structures (Cole, 1905). Hard hagfish cartilages such as the nasal and auditory capsule were found to have an ECM that stained orange/red with eosin, while soft cartilages such as the branchial arches had an ECM that stained blue with hematoxylin (Robson et al., 2000). Results from the present investigation demonstrated that hematoxylin/eosin staining of lamprey cartilages gave an identical hard–soft staining pattern. Thus, while mammalian cartilage ECMs (bovine auricular cartilage) typically displayed both hematoxylin and eosin staining (Fig. 4C), the cartilages from jawless craniates stain differently, suggesting that variation at the molecular level gives rise to differentiation at the structural level. It turns out that an underlying similarity in ECM fibril primary structure can be associated with hard and soft cartilage groups. Acidophilic hard cartilages (orange/red stain) contain a larger proportion of basic amino acids, while basophilic soft cartilages (blue stain) contain a larger proportion of acidic amino acids. For example, hagfish contain more basic amino acids (e.g. histidine and tyrosine) in their hard cartilages than in their soft cartilages and this is also true for hard and soft lamprey cartilages (Robson et al., 1997, 2000).

Although lamprey annular cartilage was not found to stiffen with age, lamprey pericardial cartilage clearly does. The mean *E* of aged pericardial cartilage was found to be statistically larger than the mean *E* of young and aged annular cartilage, young pericardial cartilage, as well as bovine auricular cartilage tested in tension and compression. Since lamprey cartilage has demonstrated the ability to calcify *in vitro* (Langille and Hall, 1993), the 'crisp' consistency of aged lamprey pericardial cartilage suggested a possible deposition of calcium within the cartilage ECM, within the chondrocytes or, possibly, within the inter-fibrillar spaces of perichondrial collagen fibers. However, staining with alizarin red was inconclusive; young and aged pericardial cartilages gave staining patterns that were virtually identical (both with and without EDTA treatment). In addition, examination of lamprey pericardial cartilage perichondria *via* transmission electron microscopy also failed to uncover evidence of mineralization, as no electron-dense aggregations were found within collagen inter- or intrafibrillar spaces of perichondria. Thus, while we cannot completely rule out the possibility of mineralization in aged pericardial cartilage (i.e. free ion mineralization), we cannot substantiate its contribution to an increase in the tissue's stiffness. Nevertheless, it does seem likely that the determinant(s) of increased stiffness is in some way associated with the condition of the perichondrial tissue. Electron microscopical observations revealed degeneration in the mesothelium of the aged pericardial cartilage's outer perichondrium and this is probably linked to the age-associated degradation of the liver, which in turn results in a large portion of metabolic waste being released to the surrounding environment (i.e. the pericardial cartilage's outer perichondrium).

Conclusions

Results of this investigation have confirmed that both lamprey annular and pericardial cartilages are viscoelastic structures with different equilibrium stiffnesses, as indicated by variations in tissue morphology and load orientation. Despite mechanical and functional differences, lamprey annular and pericardial cartilages demonstrate *E* and relaxation properties similar to those of mammalian cartilages. In light of this, lamprey cartilages should prove to be useful models in the elucidation of fundamental principles that modulate vertebrate cartilage structure–function relationships *in vitro* and *in vivo*.

This work was supported by an NSERC (Canada) grant to G. M. Wright. The authors thank two anonymous reviewers for insightful suggestions on this manuscript.

References

Aitken, G. K., Bourne, R. B., Finlay, J. B., Rorabeck, C. H. and Andreae, P. R. (1985). Indentation stiffness of the cancellous bone in the distal human tibia. *Clin. Orthop.* **201**, 264-270.

Akizuki, S., Mow, V. C., Muller, F., Pita, J. C., Howell, D. S. and Manicourt, D. H. (1986). Tensile properties of human knee joint cartilage. I. Influence of ionic conditions, weight bearing, and fibrillation on the tensile modulus. *J. Orthop. Res.* **4**, 379-392.

Cole, F. J. (1905). A monograph on the general morphology of the myxinoid fishes, based on a study of *Myxine*. 1. The anatomy of the skeleton. *Trans. R. Soc. Edinburgh* **41**, 749-791.

Comper, W. D. and Lyons, K. C. (1993). Non-electrostatic factors govern the hydrodynamic properties of articular cartilage proteoglycan. *Biochem. J.* **289**, 543-547.

Comper, W. D. and Zamparo, O. (1990). Hydrodynamic properties of connective-tissue polysaccharides. *Biochem. J.* **269**, 561-564.

Courtland, H.-W. (2001). Equilibrium mechanical properties of two noncollagenous cartilages in the sea lamprey *Petromyzon marinus*. *M.Sc. Thesis.* University of Prince Edward Island, Charlottetown, PE, Canada.

Craatz, S., Weiss, J. and Schmidt, W. (1999). Histologic-histochemical and immunocytochemical investigations of cartilage canals in human rib cartilage. *Anat. Anz.* **181**, 359-363.

Dimery, N. J., Alexander, R. McN. and Deyst, K. A. (1985). Mechanics of the ligamentum nuchae of some artiodactyls. *J. Zool.* **206A**, 341-351.

Freeman, P. M., Natarjan, R. N., Kimura, J. H. and Andriacchi, T. P. (1994). Chondrocyte cells respond mechanically to compressive loads. *J. Orthop. Res.* **12**, 311-320.

Guilak, F. (2000). The deformation behavior and viscoelastic properties of chondrocytes in articular cartilage. *Biorheology* **37**, 27-44.

Hamaide, A., Arnoczky, S. P., Ciarelli, M. J. and Gardner, K. (1998). Effects of age and location on the biomechanical and biochemical properties of canine tracheal ring cartilage in dogs. *Am. J. Vet. Res.* **59**, 18-22.

Hubbs, C. L. and Potter, I. C. (1971). Distribution, phylogeny and taxonomy. In *The Biology of Lampreys*, vol. 1 (ed. M. W. Hardisty and I. C. Potter), pp. 1-5. London: Academic Press.

Jurvelin, J. S., Buschmann, M. D. and Hunziker, E. B. (1997). Optical and mechanical determination of Poisson's ratio of adult bovine humeral articular cartilage. *J. Biomech.* **30**, 235-241.

Langille, R. M. and Hall, B. K. (1993). Calcification of cartilage from the lamprey *Petromyzon marinus* (L.) in vitro. *Acta. Zool.* **74**, 31-41.

Mansour, J. M. and Mow, V. C. (1976). The permeability of articular cartilage under compressive strain and at high pressures. *J. Bone Joint Surg.* **58**, 509-516.

Maroudas, A. (1979). Physicochemical properties of articular cartilage. In *Adult Articular Cartilage*, 2nd edition (ed. M. A. R. Freeman), pp. 215-290. Turnbridge Wells, UK: Pitman Medical.

Mow, V. C., Proctor, C. S. and Kelly, M. A. (1989). Biomechanics of articular cartilage. In *Cartilage: Biomechanics of the Musculoskeletal System*, 2nd edition (ed. M. Nordin and V. H. Frankel), pp. 31-58. Philadelphia: Lea and Febiger.

Mow, V. C., Kuei, S. C., Lai, W. M. and Armstrong, C. G. (1980). Biphasic creep and stress relaxation of articular cartilage in compression? Theory and experiments. *J. Biomech. Eng.* **102**, 73-84.

Oloyede, A. and Broom, N. (1996). The biomechanics of cartilage load-carriage. *Conn. Tiss. Res.* **34**, 119-143.

Presnell, J. K. and Schreibman, M. P. (1997). Staining pigments and minerals. In *Humason's Animal Tissue Techniques*, 5th edition (ed. J. K. Presnell and M. P. Schreibman), pp. 223-224. Baltimore: Johns Hopkins University Press.

Proctor, C. S., Schmidt, R. R., Whipple, R. R., Kelly, M. A. and Mow, V. C. (1989). Material properties of the normal medial bovine meniscus. *J. Orthop. Res.* **7**, 771-782.

Prophet, E. B., Mills, B., Arrington, J. B. and Sobin, L. H. (ed.) (1992). *Armed Forces Institute of Pathology: Laboratory Methods in Histotechnology*. Washington, DC: American Registry of Pathology.

Quinn, P., Barros, C. and Whittingham, D. G. (1982). Preservation of hamster oocytes to assay the fertilization capacity of human spermatozoa. *J. Reprod. Fertil.* **66**, 161-168.

Rains, J. K., Bert, J. L., Roberts, C. R. and Pare, P. D. (1992). Mechanical properties of human tracheal cartilage. *J. Appl. Physiol.* **72**, 219-225.

Roberts, C. R., Rains, J. K., Paré, P. D., Walker, D. C., Wiggs, B. and Bert, J. L. (1998). Ultrastructure and tensile properties of human tracheal cartilage. *J. Biomech.* **31**, 81-86.

Robson, P., Wright, G. M. and Keeley, F. W. (2000). Distinct non-collagen based cartilages comprising the endoskeleton of the Atlantic hagfish, *Myxine glutinosa*. *Anat. Embryol.* **202**, 281-290.

Robson, P., Wright, G. M., Youson, J. H. and Keeley, F. W. (1997). A family of non-collagen-based cartilages in the skeleton of the sea lamprey, *Petromyzon marinus*. *Comp. Biochem. Physiol. B* **118**, 71-78.

Robson, P., Wright, G. M., Sitarz, E., Maiti, A., Rawat, M., Youson, J. H. and Keeley, F. W. (1993). Characterization of lamprin, an unusual matrix protein from lamprey cartilage. *J. Biol. Chem.* **268**, 1440-1447.

Rovainen, C. M. (1973). Projections of individual axons in lamprey spinal cord determined by tracings through serial sections. *J. Comp. Neurol.* **149**, 193-201.

Schmidt, M. B., Schoonbeck, J. M., Mow, V. C., Eyre, D. R. and Chun, L. E. (1987). The relationship between collagen crosslinking and the tensile properties of articular cartilage. *Trans. Orthop. Res. Soc.* **12**, 134.

Schmidt, M. B., Mow, V. C., Chun, L. E. and Eyre, D. R. (1990). Effects of proteoglycan extraction on the tensile behavior of articular cartilage. *J. Orthop. Res.* **8**, 353-363.

Serafini-Fracassini, A. and Smith, J. W. (1974a). Glycosaminoglycans and proteoglycans. In *The Structure and Biochemistry of Cartilage* (ed. A. Serafini-Fracassini and J. W. Smith), pp. 64-112. London: Churchill Livingstone.

Serafini-Fracassini, A. and Smith, J. W. (1974b). Elastic cartilage. In *The Structure and Biochemistry of Cartilage* (ed. A. Serafini-Fracassini and J. W. Smith), pp. 220-228. London: Churchill Livingstone.

Shingleton, W. D., Mackie, E. J., Cawston, T. E. and Jeffcott, L. B. (1997). Cartilage canals in equine articular/epiphyseal growth cartilage and a possible association with dyschondroplasia. *Equine Vet. J.* **29**, 360-364.

Stockwell, R. A. (1979). *Biology of Cartilage Cells*. Cambridge: Cambridge University Press.

Vogel, S. (1988). A matter of materials. In *Life's Devices* (ed. S. Vogel), pp. 177-200. Princeton: Princeton University Press.

Wong, M., Ponticiello, M., Kovanen, V. and Jurvelin, J. S. (2000). Volumetric changes of articular cartilage during stress relaxation in unconfined compression. *J. Biomech.* **33**, 1049-1054.

Wright, G. M. and Youson, J. H. (1983). Ultrastructure of cartilage from young adult sea lamprey, *Petromyzon marinus* L: a new type of vertebrate cartilage. *Am. J. Anat.* **167**, 59-70.

Wright, G. M., Keeley, F. W. and Robson, P. (2001). The unusual cartilaginous tissues of jawless craniates, cephalochordates and invertebrates. *Cell Tissue. Res.* **304**, 165-174.

Wright, G. M., Keeley, F. W. and Youson, J. H. (1983). Lamprin: a new vertebrate protein comprising the major structural protein of adult lamprey cartilage. *Experientia* **39**, 495-497.

Wright, G. M., Armstrong, L. A., Jacques, A. M. and Youson, J. H. (1988). Trabecular, nasal, branchial, and pericardial cartilages in the sea lamprey, *Petromyzon marinus*: fine structure and immunohistochemical detection of elastin. *Am. J. Anat.* **182**, 1-15.

Yao, J. Q. and Seedhom, B. B. (1993). Mechanical conditioning of articular cartilage to prevalent stresses. *Brit. J. Rheum.* **32**, 956-965.